



Dynamical behavior of multiwave interaction solutions for the (3+1)-dimensional Kadomtsev-Petviashvili-Bogoyavlensky-Konopelchenko equation

Peng-Fei Han · Taogetusang Bao

Received: 6 October 2022 / Accepted: 8 November 2022 / Published online: 23 November 2022
© The Author(s), under exclusive licence to Springer Nature B.V. 2022

Abstract The (3+1)-dimensional Kadomtsev-Petviashvili-Bogoyavlensky-Konopelchenko equation is used to simulate the evolution of shallow water waves with weakly nonlinear restorative forces and waves in a strong magnetic medium, as well as ion acoustic waves and stratified ocean internal waves in incompressible fluids. The bilinear representation, Bäcklund transformation, Lax pair and infinite conservation laws of the equation are systematically constructed by using the Bell polynomial method. Based on the Hirota bilinear method and some propositions, several new analytic solutions are studied, including the hybrid solutions among the lump waves and periodic waves, mixed solutions between the lump waves and periodic waves, mixed solutions between periodic waves. The dynamic behaviors of these analytical solutions are studied by means of three-dimensional diagrams, and some new structures and properties of waves are found. The research results provide a new method for us to explore the model. The obtained results can be widely used to report various interesting physical phenomena in the

field of shallow water waves, fluid mechanics, ocean dynamics and other similar fields.

Keywords (3+1)-dimensional Kadomtsev-Petviashvili-Bogoyavlensky-Konopelchenko equation · Bell polynomial method · Bäcklund transformation · Hirota bilinear method · Infinite conservation laws · Periodic waves

1 Introduction

With the rapid development of modern science and technology, soliton theory has attracted wide attention in the fields of oceanography, plasma physics, condensed state physics and atmospheric oceanography [1–8]. Nonlinear evolution equations can simulate many complex physical phenomena observed in nature [9–12]. Therefore, the study of analytical solutions of nonlinear evolution equations has become one of the important research topics in nonlinear science [13, 14]. People have been committed to find the analytical solutions for nonlinear evolution equations, including the lump solutions [15, 16], rogue wave solutions [17–20], rational solutions [21, 22], periodic solutions [23], breathers [24–26], bifurcation solitons [27] and so on. In order to explore the analytical solutions of nonlinear evolution equations and to figure out these phenomena in nature, many methods have been studied, such as the inverse scattering transformation method [28], nonlocal symmetry method [29, 30], Riemann–Hilbert

P.-F. Han · T. Bao (✉)
College of Mathematics Science, Inner Mongolia Normal University, Huhhot 010022, People's Republic of China
e-mail: tgts@imnu.edu.cn

P.-F. Han
e-mail: 448024030@qq.com

P.-F. Han · T. Bao
Center for Applied Mathematics Inner Mongolia, Huhhot 010022, People's Republic of China

method [31,32], Lie group method [33–37], Hirota bilinear method [38–40], long wave limit approach [41,42], Darboux transformation [43,44] and many others.

In this study, we will focus our attention on the following (3+1)-dimensional Kadomtsev-Petviashvili-Bogoyavlensky-Konopelchenko equation to simulate the evolution of shallow water waves with weakly non-linear restorative forces and waves in a strong magnetic medium, as well as ion acoustic waves and stratified ocean internal waves in incompressible fluids.

$$\begin{aligned}
 &h_1u_{xxxx} + h_2u_{xxxxy} + h_3u_{xxxz} + h_4u_xu_{xx} \\
 &+ h_5(u_xu_y)_x + h_6(u_xu_z)_x \\
 &+ h_7u_{xt} + h_8u_{yt} + h_9u_{zt} \\
 &+ h_{10}u_{xz} + h_{11}u_{yz} + h_{12}u_{zz} = 0, \tag{1}
 \end{aligned}$$

where $u = u(x, y, z, t)$ is a function of the three scaled spatial variables x, y, z and the temporal variable t , with the parameters of $h_i (i = 1, 2, \dots, 12)$ are real constants. Changing the parameters of Eq. (1) can be simplified into the following equations.

(1) When we restrict u to being z -independent and $h_7 = 1, h_3 = h_6 = h_8 = h_9 = h_{10} = h_{11} = h_{12} = 0$. Equation (1) has been reduced to the (2+1)-dimensional generalized Bogoyavlensky-Konopelchenko equation [45]

$$u_{xt} + h_1u_{xxxx} + h_2u_{xxxxy} + h_4u_xu_{xx} + h_5(u_xu_y)_x = 0, \tag{2}$$

which can be used to describe the interaction of a Riemann wave propagating along y -axis and a long wave propagating along x -axis. The complete integrability of Eq. (2) is studied, and the periodic wave solutions and soliton solutions are obtained [45].

(2) By plugging $h_1 = h_4 = 0, h_2 = 1, h_5 = 3, h_6 = 3h_3$ in Eq. (1), simplify the generalized (3+1)-dimensional Kadomtsev-Petviashvili equation [46]

$$\begin{aligned}
 &u_{xxxxy} + 3(u_xu_y)_x + h_3u_{xxxz} + 3h_3(u_xu_z)_x \\
 &+ h_7u_{xt} + h_8u_{yt} + h_9u_{zt} \\
 &+ h_{10}u_{xz} + h_{11}u_{yz} + h_{12}u_{zz} = 0, \tag{3}
 \end{aligned}$$

the lump and lump strip solutions of Eq. (3) are obtained based on the Hirota bilinear method [46]. In addition, the breather and lump solutions, shock wave solutions and travelling-wave solutions of Eq. (3) are also widely studied [47].

(3) For the parameter value case of $h_2 = h_3 = h_8 = h_9 = 1, h_5 = h_6 = -3, h_1 = h_4 = h_7 =$

$h_{10} = h_{11} = h_{12} = 0$. Equation (1) can be reduced to the (3+1)-dimensional Boiti-Leon-Manna-Pempinelli equation [48]

$$u_{yt} + u_{zt} + u_{xxxxy} + u_{xxxz} - 3(u_xu_y)_x - 3(u_xu_z)_x = 0, \tag{4}$$

which describes the evolutions of ion acoustic wave and stratified ocean internal wave in incompressible fluid [49]. Breather, rational solutions, lump-kink solutions and localized excitation solutions as well as new non-traveling wave solutions of Eq. (4) were constructed [49–51].

(4) For the parameter value case of $h_1 = h_2 = h_3 = \lambda_1, h_7 = h_8 = h_9 = 1, h_{10} = h_{11} = h_{12} = 0, h_4 = 2h_5 = 2h_6 = 2\lambda_2$. Equation (1) has been reduced to a new (3+1)-dimensional Boiti-Leon-Manna-Pempinelli equation with constant coefficients [52]

$$\begin{aligned}
 &u_{xt} + u_{yt} + u_{zt} + \lambda_1(u_{xxxx} + u_{xxxxy} + u_{xxxz}) \\
 &+ \lambda_2[u_x(u_x + u_y + u_z)]_x = 0, \tag{5}
 \end{aligned}$$

which describes the wave propagation in incompressible fluid [52]. Lump solutions, interaction solutions between lump wave and solitary waves, breather solutions and N -soliton solutions of Eq. (5) were studied [53,54].

(5) Setting $h_2 = 1, h_5 = 3, h_8 = 2, h_{10} = -3, h_1 = h_3 = h_4 = h_6 = h_7 = h_9 = h_{11} = h_{12} = 0$ in Eq. (1) gives the (3+1)-dimensional Jimbo-Miwa equation [55]

$$u_{xxxxy} + 3(u_xu_y)_x + 2u_{yt} - 3u_{xz} = 0, \tag{6}$$

which comes from the second equation in the well-known KP hierarchy of integrable systems and can be used to describe certain interesting (3+1)-dimensional waves in physics [55]. Exact cross kink-wave and periodic solitary-wave solutions of the (3+1)-dimensional Jimbo-Miwa equation are studied by using the Hirota bilinear method [56]. Wazwaz proposed the following two extended (3+1)-dimensional Jimbo-Miwa equations [57]

$$\begin{aligned}
 &u_{xxxxy} + 3(u_xu_y)_x + 2(u_{xt} + u_{yt} + u_{zt}) - 3u_{xz} = 0, \\
 &u_{xxxxy} + 3(u_xu_y)_x + 2u_{yt} - 3(u_{xz} + u_{yz} + u_{zz}) = 0, \tag{7}
 \end{aligned}$$

lump solutions, lump-kink solutions, high-order lumps, high-order breathers and hybrid solutions of Eq. (7) are derived [58,59]. The analytical solutions of the above special equations have been extensively studied, and

the analysis of these solutions has greatly enriched the soliton theory.

In the following, we mainly use the binary Bell polynomial method to study the Bäcklund transformation, Lax pair and infinite conservation laws of Eq. (1). The main purpose of this paper is to construct some new multiwave interaction solutions by using the Hirota bilinear method through the transformation of nonzero seed solutions, including the hybrid solutions among the lump waves and periodic waves, mixed solutions between the lump waves and periodic waves, mixed solutions between periodic waves. Then, several new analytic solutions are obtained by constructing new auxiliary functions which include a few free functions with respect to t . These new types of mixed solutions greatly enrich the types of analytical solutions, and they can well explain some nonlinear phenomena. As far as the authors know, the multiwave interaction solutions and relevant dynamical behaviors of Eq. (1) have not been reported before. Next, the dynamic characteristics of the multiwave interaction solutions are analyzed through appropriate parameters and functions to better simulate some new physical phenomena.

2 Bilinear representation, Lax pair, Bäcklund transformation and infinite conservation laws

Hirota bilinear method and binary Bell polynomial method are the most effective and direct tools to study the integrability of nonlinear evolution equations. Bilinear representation, Bäcklund transformation, Lax pair and infinite conservation laws of Eq. (1) are systematically constructed by using the binary Bell polynomial method.

2.1 Bilinear representation

Consider the following integrable constraints

$$\begin{aligned}
 h_2 = h_3 = h_1, h_4 = 6h_1, h_5 = h_6 = 3h_1, \\
 h_7 = h_8 = h_9 = h_{10} = h_{11} = h_{12} = 1,
 \end{aligned}
 \tag{8}$$

inserting the variable transformation $u = p_x$ into Eq. (1), integrating it with respect to x once and taking the integration constant as zero, the following equation can be obtained:

$$\begin{aligned}
 E(p) = h_1(p_{xxxx} + 3p_{xx}^2 + p_{xxy} \\
 + 3p_{xx}p_{xy} + p_{xxxz} + 3p_{xx}p_{xz}) + p_{xt} + p_{yt}
 \end{aligned}$$

$$+ p_{zt} + p_{xz} + p_{yz} + p_{zz} = 0,
 \tag{9}$$

where the variable $p = p(x, y, z, t)$ is the function of x, y, z and t . With the help of the binary Bell polynomial method [60], Eq. (9) can be reduced to the following \mathcal{P} -polynomial system

$$\begin{aligned}
 \mathcal{P}_{xt}(p) + \mathcal{P}_{yt}(p) + \mathcal{P}_{zt}(p) + \mathcal{P}_{xz}(p) \\
 + \mathcal{P}_{yz}(p) + \mathcal{P}_{zz}(p) \\
 + h_1[\mathcal{P}_{xxx}(p) + \mathcal{P}_{xxy}(p) + \mathcal{P}_{xxz}(p)] = 0.
 \end{aligned}
 \tag{10}$$

By means of the transformation $p = 2 \ln f$, the system (10) is converted to bilinear representation

$$\begin{aligned}
 [h_1 D_x^4 + h_1 D_x^3 D_y + h_1 D_x^3 D_z + D_x D_t + D_y D_t \\
 + D_z D_t + D_x D_z + D_y D_z + D_z^2] f \cdot f = 0.
 \end{aligned}
 \tag{11}$$

2.2 Bäcklund transformation and Lax pair

Assuming that p and \bar{p} are two different solutions of Eq. (9), select the variable transformation $p = 2 \ln f$ and $\bar{p} = 2 \ln g$. Meanwhile, with the assumptions $\bar{p} - p = 2v, \bar{p} + p = 2w$, we have

$$\begin{aligned}
 E(\bar{p}) - E(p) = 2h_1(v_{xxxx} + 6v_{xx}w_{xx} + v_{xxy} \\
 + 3v_{xx}w_{xy} + 3w_{xx}v_{xy} + v_{xxz} \\
 + 3v_{xx}w_{xz} + 3w_{xx}v_{xz}) + 2(v_{xt} \\
 + v_{yt} + v_{zt} + v_{xz} + v_{yz} + v_{zz}) = 0.
 \end{aligned}
 \tag{12}$$

With the help of the binary Bell polynomial method [60], Eq. (12) is rewritten as follows:

$$\begin{aligned}
 E(\bar{p}) - E(p) = 2\partial_x[h_1\mathcal{Y}_{xxx}(v, w) + \mathcal{Y}_t(v) \\
 + \mathcal{Y}_z(v)] + 6h_1(v_{xx}w_{xx} - v_xw_{xxx} - v_x^2v_{xx}) \\
 + 2\partial_y[h_1\mathcal{Y}_{xxx}(v, w) + \mathcal{Y}_t(v) + \mathcal{Y}_z(v)] \\
 + 6h_1(v_{xx}w_{xy} - v_xw_{xxy} - v_x^2v_{xy}) \\
 + 2\partial_z[h_1\mathcal{Y}_{xxx}(v, w) + \mathcal{Y}_t(v) + \mathcal{Y}_z(v)] \\
 + 6h_1(v_{xx}w_{xz} - v_xw_{xxz} - v_x^2v_{xz}) = 0.
 \end{aligned}
 \tag{13}$$

We introduce the appropriate constraint

$$w_{xx} + v_x^2 + w_{xy} + v_xv_y + w_{xz} + v_xv_z = \lambda v_x,
 \tag{14}$$

with λ being an arbitrary constant. With the aid of condition (14), Eq. (13) is converted to the following form:

$$\begin{aligned}
 E(\bar{p}) - E(p) = 2\partial_x[h_1\mathcal{Y}_{xxx}(v, w) + \mathcal{Y}_t(v) + \mathcal{Y}_z(v)] \\
 + 2\partial_y[h_1\mathcal{Y}_{xxx}(v, w) + \mathcal{Y}_t(v) + \mathcal{Y}_z(v)] \\
 + 2\partial_z[h_1\mathcal{Y}_{xxx}(v, w) + \mathcal{Y}_t(v) + \mathcal{Y}_z(v)] = 0.
 \end{aligned}
 \tag{15}$$

Eqs. (14) and (15) can be rewritten as a pair of linear combinations about \mathcal{Y} -polynomials [60]

$$\begin{aligned} h_1 \mathcal{Y}_{xxx}(v, w) + \mathcal{Y}_t(v) + \mathcal{Y}_z(v) &= 0, \\ \mathcal{Y}_{xx}(v, w) + \mathcal{Y}_{xy}(v, w) + \mathcal{Y}_{xz}(v, w) - \lambda \mathcal{Y}_x(v) &= 0. \end{aligned} \tag{16}$$

Due to the relationship between \mathcal{Y} -polynomials [60] and Hirota bilinear operator [61], the system (16) yields the Bäcklund transformation with the form

$$\begin{aligned} (h_1 D_x^3 + D_t + D_z) f \cdot g &= 0, \\ (D_x^2 + D_x D_y + D_x D_z - \lambda D_x) f \cdot g &= 0. \end{aligned} \tag{17}$$

Then, we suppose $v = \ln \psi$ and $w = p + \ln \psi$, Eq. (16) can be reduced to the linear system

$$\begin{aligned} h_1 \psi_{xxx} + 3h_1 u_x \psi_x + \psi_t + \psi_z &= 0, \\ \psi_{xx} + \psi_{xy} + \psi_{xz} + \psi(u_x + u_y + u_z) - \lambda \psi_x &= 0. \end{aligned} \tag{18}$$

It is easy to prove that the above system is just the Lax pair of the (3+1)-dimensional generalized Kadomtsev-Petviashvili-Bogoyavlensky-Konopelchenko equation under the constraint condition (8).

2.3 Infinite conservation laws

By introducing a new potential function $2\delta = \bar{p}_x - p_x$, Eqs. (14) and (15) can be rewritten as

$$\begin{aligned} p_{xx} + p_{xy} + p_{xz} + \delta_x + \delta_y + \delta_z + \delta^2 \\ + \delta \partial_x^{-1} \delta_y + \delta \partial_x^{-1} \delta_z - \lambda \delta &= 0, \\ \partial_x \left\{ h_1 [\delta_{xx} + \delta^3 + 3\delta(\delta_x + p_{xx})] + \partial_x^{-1} \delta_t \right\} \\ + \partial_y \left\{ h_1 [\delta_{xx} + \delta^3 + 3\delta(\delta_x + p_{xx})] + \partial_x^{-1} \delta_z \right\} \\ + \partial_z \left\{ h_1 [\delta_{xx} + \delta^3 + 3\delta(\delta_x + p_{xx})] + \delta + \partial_x^{-1} \delta_z \right\} \\ + \partial_t (\partial_x^{-1} \delta_y + \partial_x^{-1} \delta_z) &= 0. \end{aligned} \tag{19}$$

Assume that the function δ and arbitrary parameter λ are as follows:

$$\lambda = \varepsilon, \delta = \varepsilon + \sum_{n=1}^{\infty} \mathcal{I}_n(p, p_x, \dots) \varepsilon^{-n}. \tag{20}$$

Considering the first equation of Eq. (19), make the power coefficients of the parameter ε equal, and give the recursive formula of conversed densities \mathcal{I}_n .

$$\begin{aligned} \mathcal{I}_1 = -p_{xx} = -u_x, \mathcal{I}_2 = -\mathcal{I}_{1,x} = p_{xxx} = u_{xx}, \\ \partial_x^{-1} (\mathcal{I}_{n+1,x} + \mathcal{I}_{n+1,y} + \mathcal{I}_{n+1,z}) \end{aligned}$$

$$\begin{aligned} = -\mathcal{I}_{n,x} - \mathcal{I}_{n,y} - \mathcal{I}_{n,z} \\ - \sum_{k=1}^n \mathcal{I}_k (\mathcal{I}_{n-k} + \partial_x^{-1} \mathcal{I}_{n-k,y} \\ + \partial_x^{-1} \mathcal{I}_{n-k,z}), n = 2, 3, \dots \end{aligned} \tag{21}$$

By analyzing the second equation in Eq. (19), the infinite conservation laws of Eq. (1) can be composed of the following components:

$$\mathcal{I}_{n,t} + \mathcal{X}_{n,x} + \mathcal{M}_{n,y} + \mathcal{L}_{n,z} = 0, n = 1, 2, 3, \dots, \tag{22}$$

where $\mathcal{I}_n, \mathcal{X}_n, \mathcal{M}_n$ and \mathcal{L}_n are shown as

$$\mathcal{I}_n = \partial_x^{-1} (\mathcal{I}_{n,y} + \mathcal{I}_{n,z}). \tag{23}$$

$$\begin{aligned} \mathcal{X}_n = h_1 (\mathcal{I}_{n,xx} + 3\mathcal{I}_{n+1,x} + 3p_{xx} \mathcal{I}_n + 3\mathcal{I}_{n+2} \\ + 3 \sum_{k=1}^n \mathcal{I}_k \mathcal{I}_{n-k,x} + 3 \sum_{k=1}^{n+1} \mathcal{I}_k \mathcal{I}_{n+1-k} \\ + \sum_{i+j+k=n} \mathcal{I}_i \mathcal{I}_j \mathcal{I}_k) + \partial_x^{-1} \mathcal{I}_{n,t}. \end{aligned} \tag{24}$$

$$\begin{aligned} \mathcal{M}_n = h_1 (\mathcal{I}_{n,xx} + 3\mathcal{I}_{n+1,x} + 3q_{xx} \mathcal{I}_n + 3\mathcal{I}_{n+2} \\ + 3 \sum_{k=1}^n \mathcal{I}_k \mathcal{I}_{n-k,x} + 3 \sum_{k=1}^{n+1} \mathcal{I}_k \mathcal{I}_{n+1-k} \\ + \sum_{i+j+k=n} \mathcal{I}_i \mathcal{I}_j \mathcal{I}_k) + \partial_x^{-1} \mathcal{I}_{n,z}. \end{aligned} \tag{25}$$

$$\begin{aligned} \mathcal{L}_n = h_1 (\mathcal{I}_{n,xx} + 3\mathcal{I}_{n+1,x} + 3q_{xx} \mathcal{I}_n + 3\mathcal{I}_{n+2} \\ + 3 \sum_{k=1}^n \mathcal{I}_k \mathcal{I}_{n-k,x} + 3 \sum_{k=1}^{n+1} \mathcal{I}_k \mathcal{I}_{n+1-k} \\ + \sum_{i+j+k=n} \mathcal{I}_i \mathcal{I}_j \mathcal{I}_k) + \mathcal{I}_n + \partial_x^{-1} \mathcal{I}_{n,z}. \end{aligned} \tag{26}$$

3 Multiwave interaction solutions

Hybrid solutions play important role in multiple wave interactions, as a new type of soliton solutions, have been reported in many nonlinear systems [62]. In this section, we study the multiwave interaction solutions of Eq. (1) with the help of the Hirota bilinear method [61], including hybrid solutions among the lump waves and periodic waves, mixed solutions between the lump waves and periodic waves, mixed solutions between periodic waves.

3.1 Hybrid solutions among the lump waves and periodic waves

Consider the following integrable constraints

$$\begin{aligned} h_2 = h_3 = h_1, h_4 = 6h_1, h_5 = h_6 = 3h_1, \\ h_8 = h_9 = h_7, h_{11} = h_{12} = h_{10}, \end{aligned} \tag{27}$$

and through the Cole-Hopf transformation [61]

$$u = 2(\ln f)_x + u_0(t), \tag{28}$$

then the bilinear form of Eq.(1) can be written as follows:

$$[(D_x + D_y + D_z)(h_1 D_x^3 + h_7 D_t + h_{10} D_z)]f \cdot f = 0, \tag{29}$$

where $u_0(t)$ is an undetermined function of t . In order to investigate the hybrid solutions among the lump waves and periodic waves of Eq. (1), we assume some test functions composed of N multiple functions and M arbitrary elementary functions.

$$\begin{aligned} f_A = \alpha_0(t) + \sum_{i=1}^N k_i(t)[\alpha_i(t)x + \beta_i(t)y \\ + \gamma_i(t)z + \omega_i(t)]^{n_i} + \sum_{j=1}^M r_j(t)\Delta_j^{\rho_j} \\ [m_j(t)x + n_j(t)y + p_j(t)z + q_j(t)], \end{aligned} \tag{30}$$

where $\alpha_0(t), k_i(t), \alpha_i(t), \beta_i(t), \gamma_i(t), \omega_i(t), r_j(t), m_j(t), n_j(t), p_j(t)$ and $q_j(t)$ are undetermined functions about t , with n_i and ρ_j are integers, N and M are positive integers, Δ_j represents any elementary function.

Proposition 1 *When these test functions (30) meet the following constraints, then these test functions (30) are the solutions of the bilinear equation (29).*

$$\alpha_i(t) + \beta_i(t) + \gamma_i(t) = 0, m_j(t) + n_j(t) + p_j(t) = 0. \tag{31}$$

We have successfully studied the superposition behaviors between lump solutions and different elementary functions. Hybrid solutions among the lump waves and periodic waves contain various test functions that have been studied, including the lump solutions [63], the mixed lump stripe solutions [64], the interaction solutions between one lump wave and multi-kink waves [65], the mixed lump-kink solutions [66] and some others. The extensive study of these different types of solutions enriches the physical phenomena

in nature, the study of variable coefficient solutions is more helpful to discover new dynamic behaviors. Analytical solutions reflect many nonlinear phenomena in physics, such as the fusion and fission of solitons, the annihilation of solitons and so on. Some solutions are selected below to study the new dynamic behavior of the hybrid solutions among the lump waves and periodic waves.

Case 1.1 In the case of $\beta_1(t) = -\alpha_1(t) - \gamma_1(t), \gamma_2(t) = -\alpha_2(t) - \beta_2(t)$ are selected in the constraint conditions (31) and inserting $N = \eta_1 = \eta_2 = 2$ into the test functions (30), we attain

$$\begin{aligned} f_{A1} = \alpha_0(t) + k_1(t)[\alpha_1(t)(x - y) + \gamma_1(t)(z - y) + \omega_1(t)]^2 \\ + k_2(t)[\alpha_2(t)(x - z) + \beta_2(t)(y - z) + \omega_2(t)]^2. \end{aligned} \tag{32}$$

Inserting the test function (32) into transformation (28), the periodic double lump waves solution u_{A1} is described by three-dimensional surfaces, x -curve and t -curve plots in Figs. 1a,b,c, y -curve and t -curve plots in Figs. 1d,e,f. From Fig. 1 a, we found that the double lumps in the periodic double lump waves solution were composed of two peaks on both sides of the horizontal plane and two valleys on both sides of the horizontal plane, and their shapes presented a ∇ -shape. With the change of parameters, the periodic double lump waves solution moves along the positive direction of the x -axis, and the amplitude does not change during the whole process. However, it is observed in Fig. 1b that two adjacent lump waves collide with each other and move in opposite directions, and the distance between them gradually increases. Subsequently, in Fig. 1c, it was found that the double lump waves reached a stable state, and then presented a \wedge -shape. Similarly, the adjacent lump waves collision process has similar results in Figs. 1d,e,f. The periodic double lump waves move along the positive direction of the y -axis. Compared with Figs. 1a,b,c, it is found that the velocity along the y -axis is significantly faster than that along the x -axis.

Case 1.2 If $\alpha_1(t) = -\beta_1(t) - \gamma_1(t), \gamma_2(t) = -\alpha_2(t) - \beta_2(t), m_1(t) = -n_1(t) - p_1(t), n_2(t) = -m_2(t) - p_2(t)$ are selected in the constraint conditions (31), and $N = M = \eta_1 = \eta_2 = 2, \rho_1 = \rho_2 = 1, \Delta_1 = \Delta_2 = \cosh$ are inserted into the test functions (30), we get

$$\begin{aligned} f_{A2} = \alpha_0(t) + k_1(t)[\beta_1(t)(y - x) \\ + \gamma_1(t)(z - x) + \omega_1(t)]^2 \\ + k_2(t)[\alpha_2(t)(x - z) \end{aligned}$$

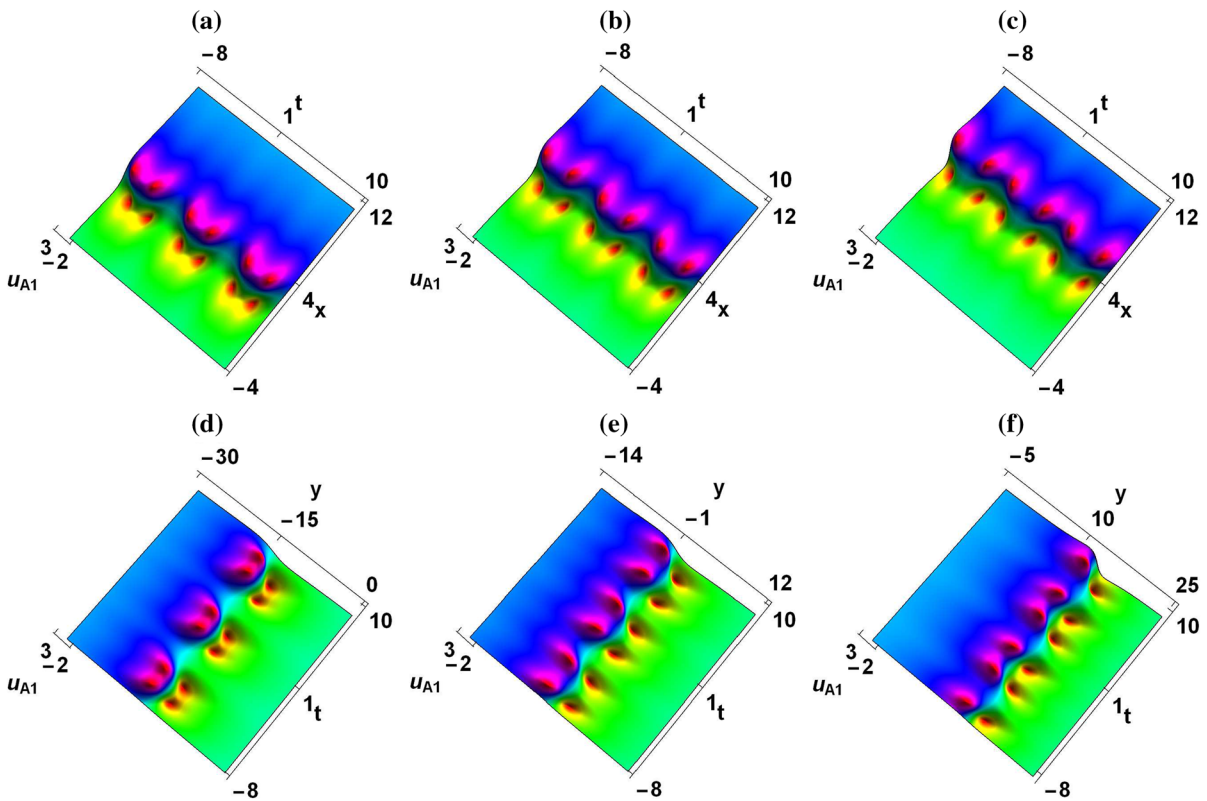


Fig. 1 (Color online) Periodic double lump waves solution by choosing parameters as $u_0(t) = 0.5, \alpha_0(t) = k_1(t) = k_2(t) = 1, \alpha_1(t) = 1.2, \alpha_2(t) = -0.6, \gamma_1(t) = -0.5, \beta_2(t) =$

$0.4, \omega_1(t) = \omega_2(t) = \sin(t) + \cos(t)$. (a) $y = -4, z = 12$, (b) $y = 2, z = 6$, (c) $y = 8, z = 0$, (d) $x = -4, z = 12$, (e) $x = 2, z = 6$, and (f) $x = 8, z = 0$

$$\begin{aligned}
 & +\beta_2(t)(y - z) + \omega_2(t)]^2 \\
 & +r_1(t) \cosh[n_1(t)(y - x) \\
 & +p_1(t)(z - x) + q_1(t)] \\
 & +r_2(t) \cosh[m_2(t)(x - y) \\
 & +p_2(t)(z - y) + q_2(t)]. \tag{33}
 \end{aligned}$$

Inserting the test function (33) into transformation (28), the hybrid solution among the lump wave and two periodic waves u_{A2} is described by three-dimensional surfaces, x -curve and t -curve plots in Figs. 2 a,b,c. By choosing different parameters, the hybrid solution among the lump wave and two kink waves u_{A2} is described by three-dimensional surfaces, x -curve and y -curve plots in Figs. 2 d,e,f. Figure 2 depicts the interaction between the lump wave, two periodic waves and two kink waves. It can be seen from Fig. 2a that the

lump wave is between two periodic waves, close to the periodic wave with higher amplitude. As the parameters change, the lump wave and two periodic waves move along the positive direction of the x -axis. It is observed from Fig. 2b that the speed of two periodic waves are faster than the lump wave, and the lump wave is close to the periodic wave with low-amplitude. Then it can be seen from Fig. 2c that due to different velocities, the lump wave collides with the low-amplitude periodic wave and the amplitude decreases. It can be seen from Figs. 2 d,e,f that the lump wave and two kink waves move at a certain angle along the x -axis and y -axis, and the amplitude and shape do not change. This is because the t function is taken as a constant coefficient, the interaction phenomenon of this solution has been widely studied.

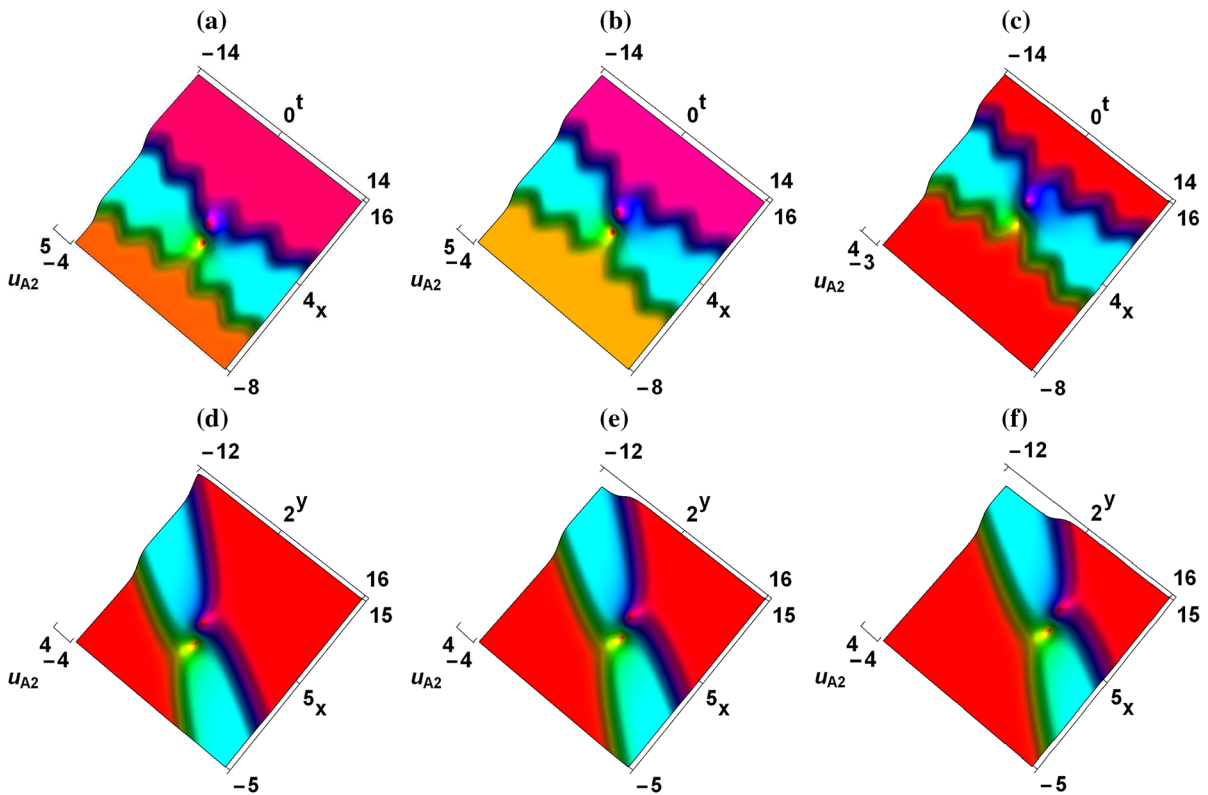


Fig. 2 (Color online) Hybrid solution among the lump wave and two periodic waves by choosing parameters as $u_0(t) = r_2(t) = n_1(t) = 0.5, \alpha_0(t) = r_1(t) = 1, k_1(t) = k_2(t) = 2, \beta_1(t) = m_2(t) = -2, \gamma_1(t) = -0.5, \alpha_2(t) = -1.6, p_1(t) = -0.7, \beta_2(t) = 1.5, p_2(t) = -0.1, \omega_1(t) = \omega_2(t) = 2t, q_1(t) = q_2(t) = \sin(t) + \cos(t)$. (a) $y = 2, z = 6$, (b) $y = z = 4$, and

(c) $y = 6, z = 2$. Hybrid solution among the lump wave and two kink waves by choosing parameters as $u_0(t) = -0.1, \alpha_0(t) = k_2(t) = q_1(t) = q_2(t) = 1, k_1(t) = 1.5, r_1(t) = 0.5, r_2(t) = 0.7, \alpha_2(t) = -1.8, \beta_2(t) = -1.4, n_1(t) = -1, m_2(t) = \gamma_1(t) = -0.7, p_1(t) = 3, p_2(t) = 0.8, \beta_1(t) = \omega_1(t) = \omega_2(t) = 2$. (d) $z = 2$, (e) $z = 4$, and (f) $z = 6$

3.2 Mixed solutions between the lump waves and periodic waves

Now, we consider the mixed solutions between the lump waves and periodic waves, which are the product form of the combination of polynomial functions and arbitrary elementary functions.

$$f_B = \left\{ a_0(t) + \sum_{i=1}^N k_i(t)[a_i(t)x + b_i(t)y + c_i(t)z + d_i(t)]^{\eta_i} + \sum_{j=1}^M s_j(t)\Delta_j^{\rho_j} [\alpha_j(t)x + \beta_j(t)y + \gamma_j(t)z + \omega_j(t)] \right\}$$

$$\times \left\{ \sum_{e=1}^E r_e(t)[m_e(t)x + n_e(t)y + p_e(t)z + q_e(t)]^{\theta_e} + m_0(t) + \sum_{l=1}^L v_l(t)\Phi_l^{\delta_l} [\sigma_l(t)x + \varpi_l(t)y + \tau_l(t)z + \chi_l(t)] \right\}, \quad (34)$$

with $a_0(t), k_i(t), a_i(t), b_i(t), c_i(t), d_i(t), s_j(t), \alpha_j(t), \beta_j(t), \gamma_j(t), \omega_j(t), r_e(t), m_e(t), n_e(t), p_e(t), q_e(t), m_0(t), v_l(t), \sigma_l(t), \varpi_l(t), \tau_l(t)$ and $\chi_l(t)$ are undetermined functions about t , N, M, E and L are positive integers, where η_i, ρ_j, θ_e and δ_l are integers, Δ_j and Φ_l are arbitrary elementary functions.

Proposition 2 *When these test functions (34) meet the following constraints, then these test functions (34) are the solutions of the bilinear equation (29).*

$$\begin{aligned}
 a_i(t) + b_i(t) + c_i(t) = 0, \alpha_j(t) + \beta_j(t) + \gamma_j(t) = 0, \\
 m_e(t) + n_e(t) + p_e(t) = 0, \sigma_l(t) + \varpi_l(t) + \tau_l(t) = 0.
 \end{aligned}
 \tag{35}$$

Mixed solutions between the lump waves and periodic waves are simulated by some parameters and special functions, which can provide some wave collisions and dynamic characteristics. Because a variety of elementary functions can be selected, the compound solutions of different functions in Reference [67] are included. This new type of solution selection has various forms, and it is possible to find some new interaction phenomena of solutions. Three new solutions are selected to study new physical phenomena.

Case 2.1 In the case of $a_1(t) = -b_1(t) - c_1(t)$, $b_2(t) = -a_2(t) - c_2(t)$, $n_1(t) = -m_1(t) - p_1(t)$, $p_2(t) = -m_2(t) - n_2(t)$ are selected in the constraint conditions (35) and inserting $N = E = \eta_1 = \eta_2 = \theta_1 = \theta_2 = 2$ into the test functions (34), we attain

$$\begin{aligned}
 f_{B1} = & \left\{ a_0(t) + k_1(t)[b_1(t)(y - x) + c_1(t)(z - x) \right. \\
 & + d_1(t)]^2 + k_2(t)[a_2(t)(x - y) \\
 & + c_2(t)(z - y) + d_2(t)]^2 \Big\} \\
 & \times \left\{ r_1(t)[m_1(t)(x - y) + p_1(t)(z - y) + q_1(t)]^2 \right. \\
 & + m_0(t) + r_2(t)[m_2(t)(x - z) \\
 & + n_2(t)(y - z) + q_2(t)]^2 \Big\}.
 \end{aligned}
 \tag{36}$$

Substituting the test function (36) into transformation (28), two lump waves solution u_{B1} is described by three-dimensional surfaces, x -curve and t -curve plots in Figs. 3a,b,c. By choosing different parameters, one lump wave solution u_{B1} is described by three-dimensional surfaces, x -curve and z -curve plots in Figs. 3d,e,f. Figures 3a,b,c show the fusion and fission of two lump waves. From Fig. 3a, it can be seen that the two lump waves have two peaks and two valleys on both sides of the horizontal plane. When the parameters are changed, the two lump waves move along the x -axis and t -axis at a certain angle, and the direction of motion is opposite. In Fig. 3b, it is observed that two lump waves collide with each other and directly fuse into one lump wave, and the amplitude is twice the original. In Fig. 3c, it can be found that two lump waves should move along the original direction, so one

lump wave is divided into two lump waves and the amplitude is restored. It can be seen from Figs. 3d,e,f that the lump wave moves at a certain angle along the x -axis and z -axis, and the amplitude and shape do not change.

Case 2.2 In the case of $b_1(t) = -a_1(t) - c_1(t)$, $c_2(t) = -a_2(t) - b_2(t)$, $\beta_1(t) = -\alpha_1(t) - \gamma_1(t)$, $p_1(t) = -m_1(t) - n_1(t)$, $n_2(t) = -m_2(t) - p_2(t)$, $\tau_1(t) = -\sigma_1(t) - \varpi_1(t)$ are selected in the constraint conditions (35) and inserting $N = E = \eta_1 = \eta_2 = \theta_1 = \theta_2 = 2$, $M = L = \rho_1 = \delta_1 = 1$, $\Delta_1 = \Phi_1 = \cosh$ into the test functions (34), we attain

$$\begin{aligned}
 f_{B2} = & \{ a_0(t) + k_1(t)[a_1(t)(x - y) \\
 & + c_1(t)(z - y) + d_1(t)]^2 \\
 & + k_2(t)[a_2(t)(x - z) + d_2(t) \\
 & + b_2(t)(y - z)]^2 + s_1(t) \cosh[\alpha_1(t)(x - y) \\
 & + \gamma_1(t)(z - y) + \omega_1(t)] \Big\} \\
 & \times \{ m_0(t) + r_1(t)[m_1(t)(x - z) + n_1(t)(y - z) + q_1(t)]^2 \\
 & + r_2(t)[m_2(t)(x - y) + p_2(t)(z - y) \\
 & + q_2(t)]^2 + v_1(t) \cosh[\sigma_1(t)(x - z) \\
 & + \varpi_1(t)(y - z) + \chi_1(t)] \Big\}.
 \end{aligned}
 \tag{37}$$

Substituting the test function (37) into transformation (28), the mixed solution between two lump periodic waves u_{B2} is described by three-dimensional surfaces, x -curve and t -curve plots in Figs. 4a,b,c. By choosing different parameters, the mixed solution between one lump wave and four kink waves u_{B2} is described by three-dimensional surfaces, y -curve and z -curve plots in Figs. 4 d,e,f. Figures 4a,b,c analyzes the mutual collision between two lump periodic waves, each lump periodic wave consists of two intersecting periodic waves and one lump wave. Figure 4 a shows that the distribution of two lump periodic waves is perpendicular to the x -axis and t -axis, and each lump wave is at the intersection of two periodic waves. With the change of parameters, it is observed in Fig. 4b that two lump periodic waves move in the opposite direction of the x -axis respectively and merge into one lump periodic wave. In Fig. 4c, the two lump periodic waves continue to move in opposite directions, and the amplitude remains unchanged during the whole process. It can be observed in Figs. 4d,e,f that the lump wave is distributed at the intersection of two kink waves with lower amplitude, and moves along the positive direction of y -axis and z -axis under the action of two kink waves with higher amplitude.

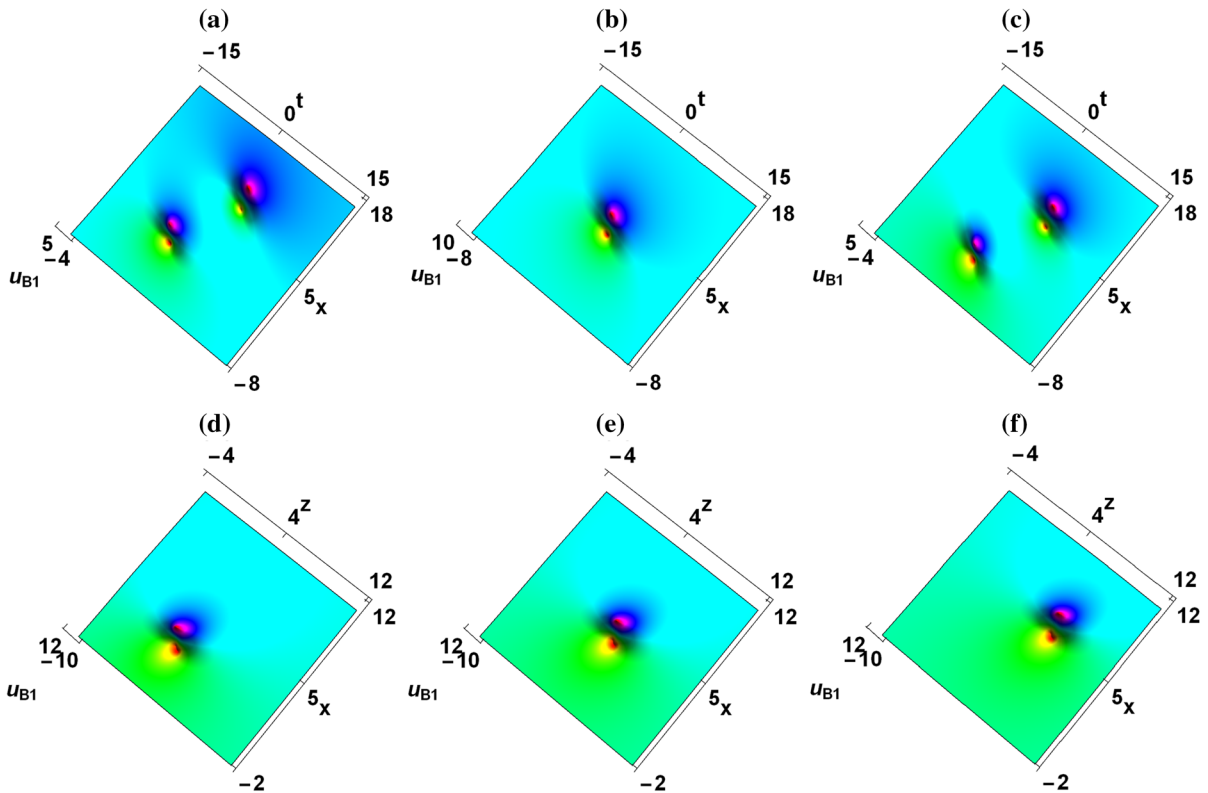


Fig. 3 (Color online) Two lump waves solution by choosing parameters as $u_0(t) = c_1(t) = 0.3, a_0(t) = m_0(t) = k_1(t) = r_1(t) = b_1(t) = 1, k_2(t) = r_2(t) = a_2(t) = p_1(t) = m_2(t) = 1.5, c_2(t) = 1.6, m_1(t) = -1, n_2(t) = 1.8, d_1(t) = d_2(t) = q_1(t) = q_2(t) = t$. (a) $y = 2, z = 6$, (b) $y = z = 4$, and (c)

$y = 6, z = 2$. One lump wave solution by choosing parameters as $u_0(t) = 0, a_0(t) = m_0(t) = d_1(t) = d_2(t) = q_1(t) = q_2(t) = k_1(t) = r_1(t) = 1, k_2(t) = r_2(t) = 1.5, b_1(t) = c_1(t) = 2, a_2(t) = c_2(t) = -2, m_1(t) = 1.8, p_1(t) = -2.2, m_2(t) = -1.3, n_2(t) = 2.5$. (d) $y = 2$, (e) $y = 4$, and (f) $y = 6$

Case 2.3 In the case of $\beta_1(t) = -\alpha_1(t) - \gamma_1(t), \gamma_2(t) = -\alpha_2(t) - \beta_2(t), \tau_1(t) = -\sigma_1(t) - \varpi_1(t), \varpi_2(t) = -\sigma_2(t) - \tau_2(t)$ are selected in the constraint conditions (35) and inserting $M = L = 2, \rho_1 = \rho_2 = \delta_1 = \delta_2 = 1, a_0(t) = m_0(t) = 0, \Delta_1 = \Delta_2 = \Phi_1 = \Phi_2 = \cosh$ into the test functions (34), we attain

$$\begin{aligned}
 f_{B3} = & \{s_1(t) \cosh[\alpha_1(t)(x - y) \\
 & + \gamma_1(t)(z - y) + \omega_1(t)] \\
 & + s_2(t) \cosh[\alpha_2(t)(x - z) \\
 & + \beta_2(t)(y - z) + \omega_2(t)]\} \\
 & \times \{v_1(t) \cosh[\sigma_1(t)(x - z) \\
 & + \varpi_1(t)(y - z) + \chi_1(t)] \\
 & + v_2(t) \cosh[\sigma_2(t)(x - y) \\
 & + \tau_2(t)(z - y) + \chi_2(t)]\}. \tag{38}
 \end{aligned}$$

Substituting the test function (38) into transformation (28), the interactions between four periodic waves u_{B3} is described by three-dimensional surfaces, x -curve and t -curve plots in Figs. 5a,b,c, z -curve and t -curve plots in Figs. 5d,e,f. Figure 5 displays the collision between four periodic waves, and studies the fusion and fission between multiple periodic waves. Four periodic waves are found in Fig. 5a, one of which has a smaller wave width compared with the other three periodic waves. One periodic wave and the other two periodic waves are distributed on both sides of the periodic wave with smaller wave width, it can be seen that the velocity of two periodic waves is obviously higher than that of one periodic wave. In Fig. 5b, it is observed that the periodic wave with smaller wave width does not move, and other periodic waves have different velocities and move in the opposite direction, so four peri-

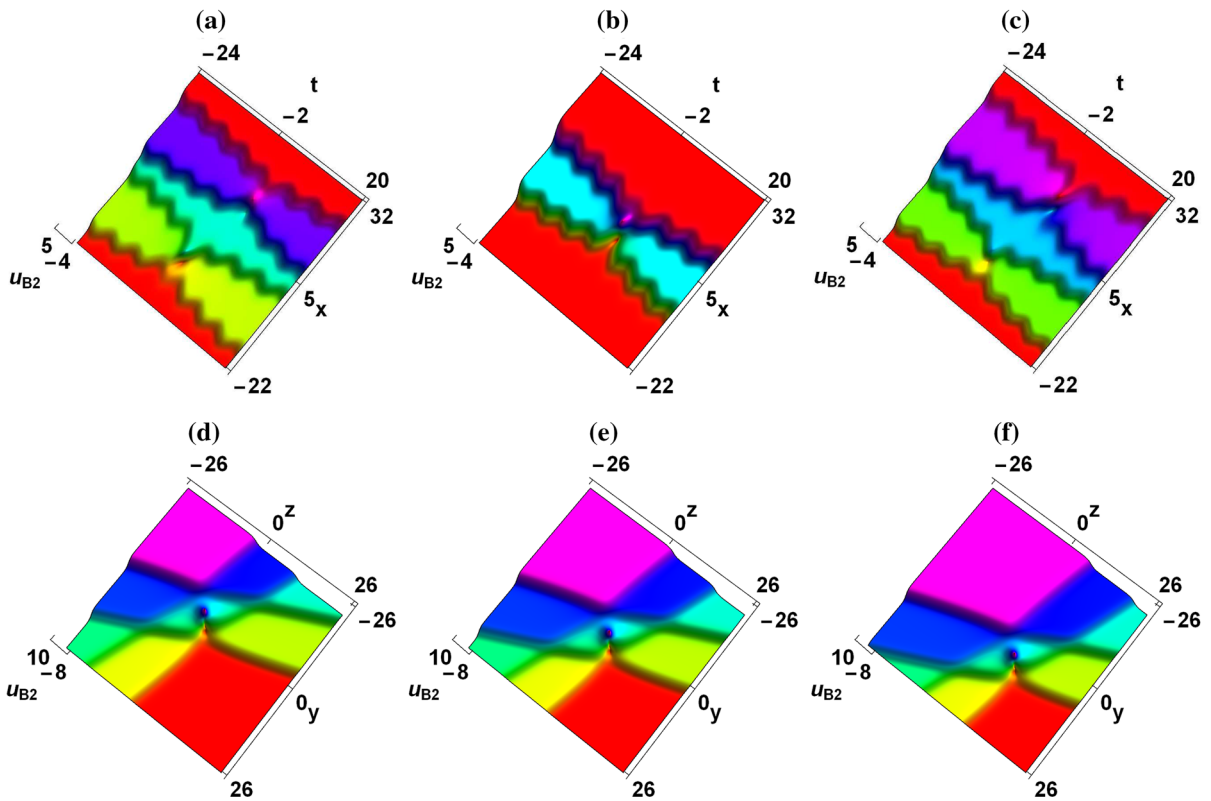


Fig. 4 (Color online) Mixed solution between two lump periodic waves by choosing parameters as $u_0(t) = v_1(t) = 0.5, a_0(t) = m_0(t) = 1, k_1(t) = k_2(t) = r_1(t) = r_2(t) = 3, s_1(t) = p_2(t) = 0.6, a_1(t) = 0.1, c_1(t) = 0.8, a_2(t) = -0.6, b_2(t) = 1.2, \alpha_1(t) = -1, \gamma_1(t) = -2.3, m_1(t) = 0.4, n_1(t) = 1.3, m_2(t) = -0.4, \varpi_1(t) = -3, \sigma_1(t) = -1.2, d_1(t) = d_2(t) = q_1(t) = q_2(t) = t, \omega_1(t) = \chi_1(t) = \cos(t)$. **(a)** $y = 2, z = 6$, **(b)** $y = z = 4$, and **(c)** $y = 6, z = 2$. Mixed solu-

tion between one lump wave and four kink waves by choosing parameters as $u_0(t) = -0.1, a_0(t) = m_0(t) = d_1(t) = d_2(t) = q_1(t) = q_2(t) = m_2(t) = 1, a_1(t) = -3, \omega_1(t) = \chi_1(t) = 2, k_1(t) = k_2(t) = r_1(t) = r_2(t) = 3, s_1(t) = v_1(t) = c_1(t) = 0.5, a_2(t) = m_1(t) = 1.2, b_2(t) = 1.6, \alpha_1(t) = -2, \gamma_1(t) = 0.6, n_1(t) = -1.4, p_2(t) = -1.2, \varpi_1(t) = 0.4, \sigma_1(t) = -1.8$. **(d)** $x = -2$, **(e)** $x = 2$, and **(f)** $x = 6$

odic waves are fused into one periodic wave. In Fig. 5c, according to the motion properties of periodic waves, they gradually split into four periodic waves and moved in the opposite direction, with no change in amplitude. A new nonlinear phenomenon appears in Figs. 5 d,e,f, where multiple periodic waves collide to produce breather solution. In Fig. 5d, two periodic waves with longer wave widths are distributed on both sides of two adjacent periodic waves with smaller wave widths. It can be seen from Fig. 5 e that two long-wave-width periodic waves move in opposite directions, respectively, and collide with two periodic waves with smaller wave widths to produce the breather solution. In Fig. 5f, it is observed that the amplitude of these four periodic

waves changes, and the direction is opposite to the original.

3.3 Mixed solutions between periodic waves

It is assumed that the mixed solutions between periodic waves have the following form

$$f_C = \left\{ \alpha_0(t) + \sum_{i=1}^N k_i(t) [\alpha_i(t)x + \beta_i(t)y + \gamma_i(t)z + \omega_i(t)]^{n_i} + \sum_{j=1}^M s_j(t) \Delta_j^{\rho_j} [m_j(t)x + n_j(t)y + p_j(t)z + q_j(t)] \right\}$$

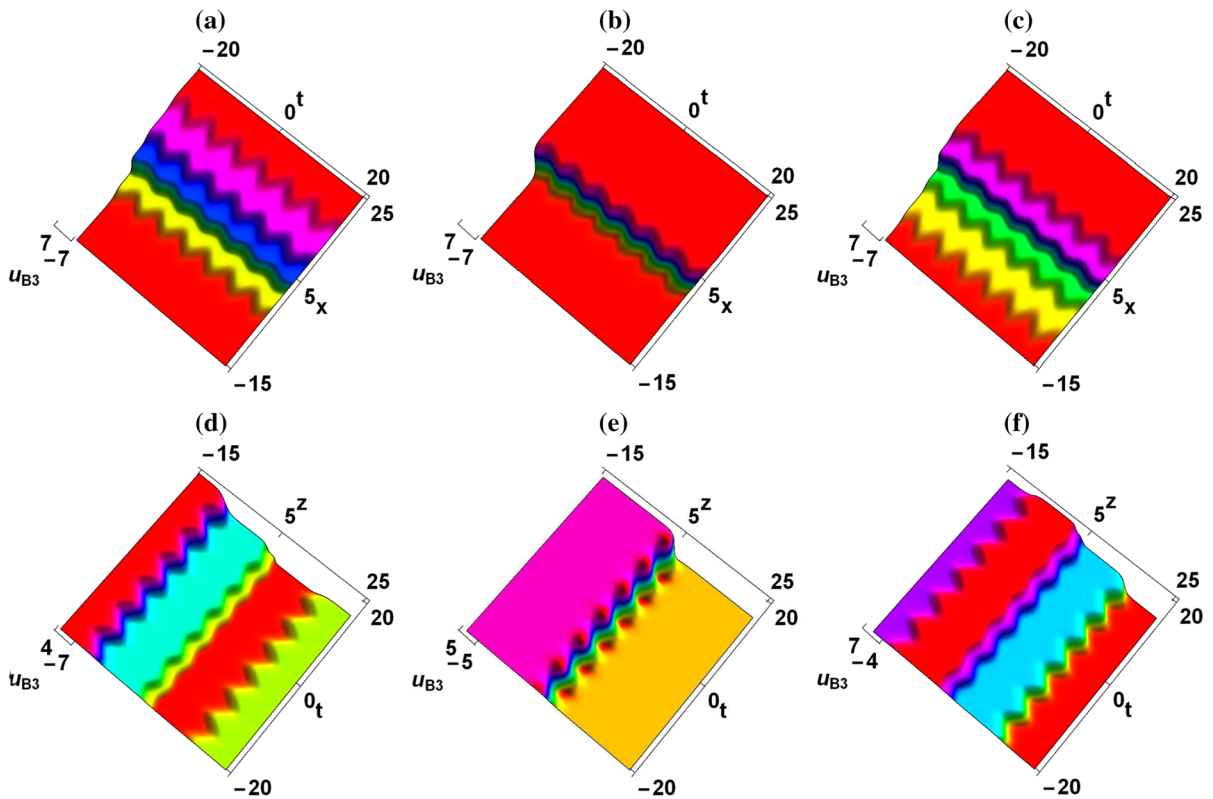


Fig. 5 (Color online) Interactions between four periodic waves by choosing parameters as $u_0(t) = 0, s_1(t) = s_2(t) = \tau_2(t) = 1.5, v_1(t) = 1.3, v_2(t) = 2, \alpha_1(t) = 0.8, \gamma_1(t) = 0.5, \alpha_2(t) = -2.2, \beta_2(t) = 0.2, \varpi_1(t) = -2.8, \sigma_1(t) = 0.1, \sigma_2(t) =$

$-1.2, \omega_1(t) = \chi_1(t) = \cos(t), \omega_2(t) = \chi_2(t) = \sin(t)$. (a) $y = 2, z = 6$, (b) $y = z = 4$, (c) $y = 6, z = 2$, (d) $x = 0, y = 8$, (e) $x = y = 4$, and (f) $x = 8, y = 0$

$$\div \left\{ a_0(t) + \sum_{e=1}^E r_e(t)[a_e(t)x + b_e(t)y + c_e(t)z + d_e(t)]^{\theta_e} + \sum_{l=1}^L v_l(t)\Phi_l^{\delta_l} [\sigma_l(t)x + \varpi_l(t)y + \tau_l(t)z + \chi_l(t)] \right\}, \quad (39)$$

with $\alpha_0(t), k_i(t), \alpha_i(t), \beta_i(t), \gamma_i(t), \omega_i(t), s_j(t), m_j(t), n_j(t), p_j(t), q_j(t), a_0(t), r_e(t), a_e(t), b_e(t), c_e(t), d_e(t), v_l(t), \sigma_l(t), \varpi_l(t), \tau_l(t)$ and $\chi_l(t)$ are undetermined functions about t , N, M, E and L are positive integers, where η_i, ρ_j, θ_e and δ_l are integers, Δ_j and Φ_l are arbitrary elementary functions.

Proposition 3 When these test functions (39) meet the following constraints, then these test functions (39) are the solutions of the bilinear Eq. (29).

$$\alpha_i(t) + \beta_i(t) + \gamma_i(t) = 0, m_j(t) + n_j(t) + p_j(t) = 0, a_e(t) + b_e(t) + c_e(t) = 0, \sigma_l(t) + \varpi_l(t) + \tau_l(t) = 0. \quad (40)$$

Mixed solutions between periodic waves are constructed according to fractional properties, and their numerator and denominator are composed of polynomial functions and any elementary functions. Because a variety of elementary functions can be selected, the hybrid solutions of fraction type in Reference [68] are included. Studying the mixed solutions between periodic waves can better analyze nonlinear phenomena in different fields. Many new forms of solutions have not been given in other documents, and more kinds of analytical solutions can be obtained.

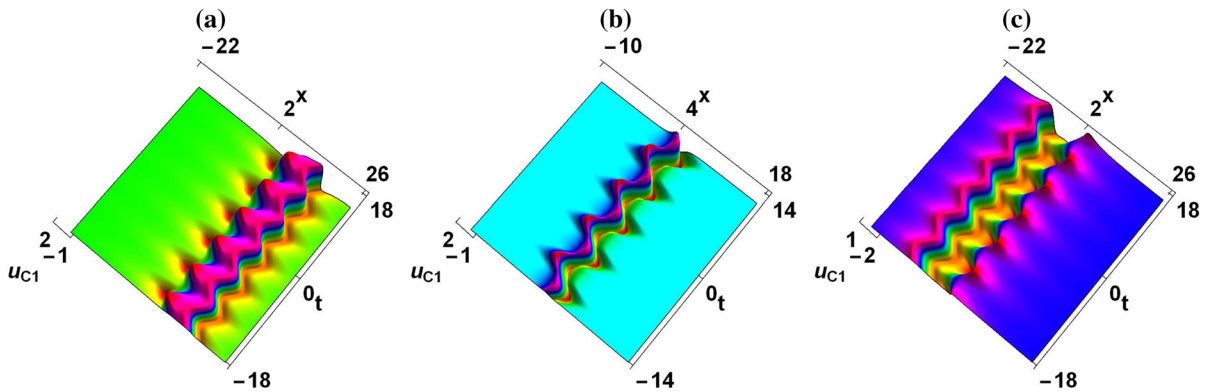


Fig. 6 (Color online) Mixed solution among periodic lump-kink wave and periodic wave by choosing parameters as $u_0(t) = 0, \alpha_0(t) = a_0(t) = k_1(t) = k_2(t) = r_1(t) = r_2(t) = \gamma_1(t) = 1, a_1(t) = a_2(t) = -0.8, c_1(t) = 3, b_2(t) = -1.6, \beta_1(t) =$

$-0.2, \alpha_2(t) = -0.1, \gamma_2(t) = 0.5, d_1(t) = d_2(t) = \omega_1(t) = \omega_2(t) = \cos(t)$. (a) $y = 2, z = 6$, (b) $y = z = 4$, and (c) $y = 6, z = 2$

Case 3.1 By plugging $\alpha_1(t) = -\beta_1(t) - \gamma_1(t), \beta_2(t) = -\alpha_2(t) - \gamma_2(t), b_1(t) = -a_1(t) - c_1(t), c_2(t) = -a_2(t) - b_2(t)$ into the constraint conditions (40) and inserting $N = E = \eta_1 = \eta_2 = \theta_1 = \theta_2 = 2$ into the test functions (39), we attain

$$f_{C1} = \{ \alpha_0(t) + k_1(t)[\beta_1(t)(y-x) + \gamma_1(t)(z-x) + \omega_1(t)]^2 + k_2(t)[\alpha_2(t)(x-y) + \gamma_2(t)(z-y) + \omega_2(t)]^2 \} \div \{ r_1(t)[a_1(t)(x-y) + c_1(t)(z-y) + d_1(t)]^2 + a_0(t) + r_2(t)[a_2(t)(x-z) + b_2(t)(y-z) + d_2(t)]^2 \}. \tag{41}$$

Substituting the test function (41) into transformation (28), we obtain the mixed solution among periodic lump-kink wave and periodic wave u_{C1} . Figure 6 analyzes the dynamic behavior of the mixed solution among periodic lump-kink wave and periodic wave, in which periodic lump-kink wave is composed of breather and periodic wave. It can be seen from Fig. 6a that both periodic lump-kink wave and periodic wave move along the negative x -axis. Because the periodic wave speed is faster than the periodic lump-kink wave speed, it collides and merges into the double periodic waves. It can be observed from Fig. 6b that the double periodic waves are composed of a periodic wave with upward direction and a periodic waves with downward direction. Then, with the different speeds of periodic lump-kink wave and periodic wave, the fission of double periodic waves causes the direction of periodic lump-kink wave and periodic wave to be different from the original, and the amplitude changes.

Case 3.2 By plugging $\beta_1(t) = -\alpha_1(t) - \gamma_1(t), \gamma_2(t) = -\alpha_2(t) - \beta_2(t), m_1(t) = -n_1(t) - p_1(t), a_1(t) = -b_1(t) - c_1(t), b_2(t) = -a_2(t) - c_2(t), \tau_1(t) = -\sigma_1(t) - \varpi_1(t)$ into the constraint conditions (40) and inserting $N = E = \eta_1 = \eta_2 = \theta_1 = \theta_2 = 2, M = L = \rho_1 = \delta_1 = 1, \Delta_1 = \Phi_1 = \cosh$ into the test functions (39), we attain

$$f_{C3} = \{ \alpha_0(t) + k_1(t)[\alpha_1(t)(x-y) + \gamma_1(t)(z-y) + \omega_1(t)]^2 + k_2(t)[\alpha_2(t)(x-z) + \omega_2(t) + \beta_2(t)(y-z)]^2 + s_1(t) \cosh[n_1(t)(y-x) + p_1(t)(z-x) + q_1(t)] \} \div \{ a_0(t) + r_1(t)[b_1(t)(y-x) + c_1(t)(z-x) + d_1(t)]^2 + r_2(t)[a_2(t)(x-y) + c_2(t)(z-y) + d_2(t)]^2 + v_1(t) \cosh[\sigma_1(t)(x-z) + \varpi_1(t)(y-z) + \chi_1(t)] \}. \tag{42}$$

By plugging the test function (42) into transformation (28), we get the two periodic lump waves u_{C2} . Figure 7 depicts the collision between two periodic lump waves, periodic lump waves are composed of periodic upward peaks and downward valleys on both sides of the horizontal plane, and their arrangement and distribution are linear. In Fig. 7a, it is found that the distribution of two periodic lump waves is perpendicular to the x -axes and t -axes, and the wave widths of the two periodic lump waves are different. It is observed from Fig. 7b that the periodic lump wave with large wave width moves along the positive direction of the x -axis and collides with the periodic lump wave with small wave width, resulting in changes in the ampli-

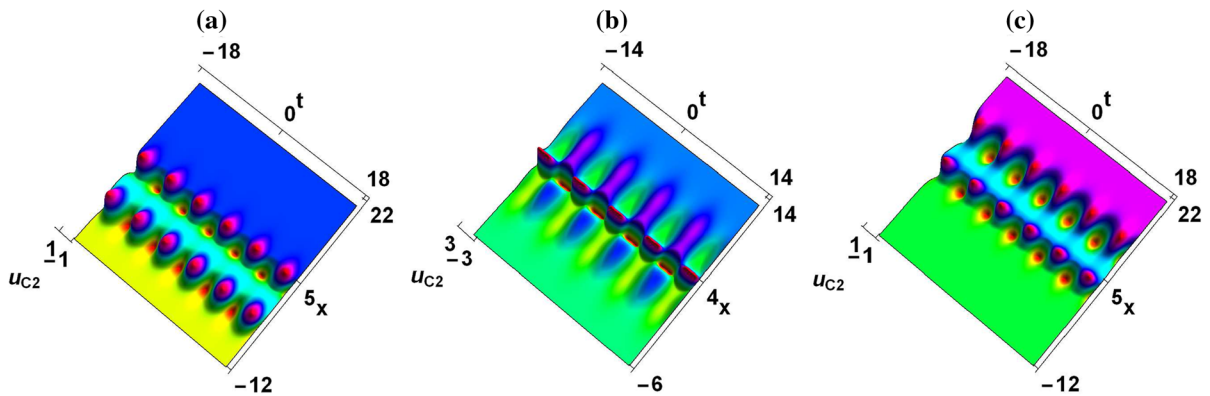


Fig. 7 (Color online) Two periodic lump waves by choosing parameters as $u_0(t) = 0, \alpha_0(t) = a_0(t) = k_1(t) = k_2(t) = r_1(t) = r_2(t) = s_1(t) = v_1(t) = 1, b_1(t) = c_2(t) = 1.5, c_1(t) = p_1(t) = -0.5, a_2(t) = -1.2, \alpha_1(t) =$

$0.8, \gamma_1(t) = -3, \alpha_2(t) = 2, \beta_2(t) = 0.7, n_1(t) = 2.1, \varpi_1(t) = -1.5, \sigma_1(t) = 1.3, d_1(t) = d_2(t) = \omega_1(t) = \omega_2(t) = q_1(t) = \chi_1(t) = \cos(t)$. (a) $y = 2, z = 6$, (b) $y = z = 4$, and (c) $y = 6, z = 2$

tude and shape of the periodic lump wave. Then it is found in Fig. 7c that the periodic lump wave with large wave width continues to move, its shape recovers but its direction changes.

4 Conclusion

In this paper, bilinear representation, Lax pair, Bäcklund transformation and infinite conservation laws are derived for the (3+1)-dimensional generalized Kadomtsev-Petviashvili-Bogoyavlensky-Konopelchenko equation based on the binary Bell polynomial method. With the help of Hirota bilinear method and some propositions, we find that the analytic solutions constructed satisfy Eq. (1). To gain a better understanding of complex wave patterns, we have drawn the three-dimensional contours simulation in Figs. 1, 2, 3, 4, 5, 6, 7 and given the detailed information of multiple mixed wave collisions. Figure 1 displays the splitting and convergence of the periodic double lump waves. Figure 2 depicts the interaction between the lump wave, two periodic waves and two kink waves. The fusion and fission of two lump waves are presented in Fig. 3. By choosing appropriate parameter values, the collision and splitting phenomenon of the two lump periodic waves, the interaction of one lump wave and four kink waves as shown in Fig. 4. The fusion and fission of multiple periodic waves are found in Fig. 5. In Fig. 6, we analyze the collision between periodic lump-kink wave and periodic wave. Figure 7 shows

the collision between two periodic lump waves. Analyzing the dynamic behavior of these mixed solutions helps us better understand the physical phenomena in the nonlinear model.

Therefore, the model proposed in this paper can effectively analyze the water wave collisions and new interaction phenomena. New mixed solutions constructed are very novel and have never been recorded in the studies before. New mixed solutions constructed in this paper are all reported for the first time for the (3+1)-dimensional generalized Kadomtsev-Petviashvili-Bogoyavlensky-Konopelchenko equation. The results show the importance and practicability of the Hirota bilinear method, the dynamic analysis of these new mixed solutions and new nonlinear phenomena can help us understand the evolution of waves in many nonlinear physical systems.

Acknowledgements The authors deeply appreciate the anonymous reviewers for their helpful and constructive suggestions, which can help improve this paper further. This work has been supported by the National Natural Science Foundation of China (Grant No. 11361040), the Fundamental Research Funds for the Inner Mongolia Normal University, China (Grant No. 2022JBZD011), the Natural Science Foundation of Inner Mongolia Autonomous Region, China (Grant No. 2020LH01008), the Graduate Students’ Scientific Research Innovation Fund Program of Inner Mongolia Normal University, China (Grant No. CXJJS19096, No. CXJJS20089) and the Graduate Research Innovation Project of Inner Mongolia Autonomous Region, China (Grant No. S20191235Z).

Data availability All data generated or analyzed during this study are included in this published article.

Declarations

Conflict of interest The authors declare that there is no conflict of interests regarding the research effort and the publication of this paper.

References

- Roth, S., Bleier, H.: Solitons in polyacetylene. *Adv. Phys.* **36**(4), 385–462 (1987)
- Ma, Y.L., Wazwaz, A.M., Li, B.Q.: New extended Kadomtsev-Petviashvili equation: multiple soliton solutions, breather, lump and interaction solutions. *Nonlinear Dyn.* **104**, 1581–1594 (2021)
- Wazwaz, A.M.: A variety of multiple-soliton solutions for the integrable (4+1)-dimensional Fokas equation. *Wave Random Complex Media* **31**, 46–56 (2021)
- Yin, H.M., Pan, Q., Chow, K.W.: Four-wave mixing and coherently coupled Schrödinger equations: Cascading processes and Fermi-Pasta-Ulam-Tsingou recurrence. *Chaos* **31**, 083117 (2021)
- Gao, X.Y.: Looking at a nonlinear inhomogeneous optical fiber through the generalized higher-order variable-coefficient Hirota equation. *Appl. Math. Lett.* **73**, 143–149 (2017)
- Dai, C.Q., Wang, Y.Y.: Coupled spatial periodic waves and solitons in the photovoltaic photorefractive crystals. *Nonlinear Dyn.* **102**, 1733–1741 (2020)
- Sun, J.Z., Li, B.Q., Ma, Y.L.: Phase complementarity and magnification effect of optical pump rogue wave and Stokes rogue wave in a transient stimulated Raman scattering system. *Optik* **269**, 169869 (2022)
- Yin, H.M., Pan, Q., Chow, K.W.: The Fermi-Pasta-Ulam-Tsingou recurrence for discrete systems: Cascading mechanism and machine learning for the Ablowitz-Ladik equation. *Commun. Nonlinear Sci. Numer. Simul.* **114**, 106664 (2022)
- Han, P.F., Taogetusang: Lump-type, breather and interaction solutions to the (3+1)-dimensional generalized KdV-type equation. *Mod. Phys. Lett. B* **34**(29), 2050329 (2020)
- Osman, M.S., Wazwaz, A.M.: A general bilinear form to generate different wave structures of solitons for a (3+1)-dimensional Boiti-Leon-Manna-Pempinelli equation. *Math. Methods Appl. Sci.* **42**, 6277–6283 (2019)
- Gao, X.Y., Guo, Y.J., Shan, W.R., Yin, H.M., Du, X.X., Yang, D.Y.: Electromagnetic waves in a ferromagnetic film. *Commun Nonlinear Sci Numer Simul.* **105**, 106066 (2022)
- Han, P.F., Bao, T.: Novel hybrid-type solutions for the (3+1)-dimensional generalized Bogoyavlensky-Konopelchenko equation with time-dependent coefficients. *Nonlinear Dyn.* **107**, 1163–1177 (2022)
- Zhang, R.F., Li, M.C., Yin, H.M.: Rogue wave solutions and the bright and dark solitons of the (3+1)-dimensional Jimbo-Miwa equation. *Nonlinear Dyn.* **103**, 1071–1079 (2021)
- Ma, H.C., Yue, S.P., Deng, A.P.: Resonance Y-shape solitons and mixed solutions for a (2+1)-dimensional generalized Caudrey-Dodd-Gibbon-Kotera-Sawada equation in fluid mechanics. *Nonlinear Dyn.* **108**, 505–519 (2022)
- Han, P.F., Bao, T.: Higher-order mixed localized wave solutions and bilinear auto-Bäcklund transformations for the (3+1)-dimensional generalized Konopelchenko-Dubrovsky-Kaup-Kupershmidt equation. *Eur. Phys. J. Plus* **137**, 216 (2022)
- Ma, W.X.: Lump solutions to the Kadomtsev-Petviashvili equation. *Phys. Lett. A* **379**, 1975–1978 (2015)
- Ohta, Y., Yang, J.K.: Rogue waves in the Davey-Stewartson I equation. *Phys. Rev. E* **86**, 036604 (2012)
- Yin, H.M., Tian, B., Zhao, X.C., Zhang, C.R., Hu, C.C.: Breather-like solitons, rogue waves, quasi-periodic/chaotic states for the surface elevation of water waves. *Nonlinear Dyn.* **97**, 21–31 (2019)
- Li, B.Q., Ma, Y.L.: Interaction properties between rogue wave and breathers to the manakov system arising from stationary self-focusing electromagnetic systems. *Chaos Solitons Fract.* **156**, 111832 (2022)
- Liu, J.G., Yang, X.J., Feng, Y.Y., Geng, L.L.: Characteristics of new type rogue waves and solitary waves to the extended (3+1)-dimensional Jimbo-Miwa equation. *J. Appl. Anal. Comput.* **11**(6), 2722–2735 (2021)
- Wang, X., Wei, J., Geng, X.G.: Rational solutions for a (3+1)-dimensional nonlinear evolution equation. *Commun Nonlinear Sci Numer Simul.* **83**, 105116 (2020)
- Liu, J.G., Yang, X.J., Wang, J.J.: A new perspective to discuss Korteweg-de Vries-like equation. *Phys. Lett. A* **451**, 128429 (2022)
- Khare, A., Saxena, A.: Periodic and hyperbolic soliton solutions of a number of nonlocal nonlinear equations. *J. Math. Phys.* **56**, 032104 (2015)
- Ma, Y.L., Wazwaz, A.M., Li, B.Q.: A new (3+1)-dimensional Kadomtsev-Petviashvili equation and its integrability, multiple-solitons, breathers and lump waves. *Math. Comput. Simulat.* **187**, 505–519 (2021)
- Yin, H.M., Tian, B., Zhang, C.R., Du, X.X., Zhao, X.C.: Optical breathers and rogue waves via the modulation instability for a higher-order generalized nonlinear Schrödinger equation in an optical fiber transmission system. *Nonlinear Dyn.* **97**, 843–852 (2019)
- Yin, H.M., Chow, K.W.: Breathers, cascading instabilities and Fermi-Pasta-Ulam-Tsingou recurrence of the derivative nonlinear Schrödinger equation: Effects of ‘self-steepening’ nonlinearity. *Phys. D* **428**, 133033 (2021)
- Ma, Y.L., Li, B.Q.: Bifurcation solitons and breathers for the nonlocal Boussinesq equations. *Appl. Math. Lett.* **124**, 107677 (2022)
- Ma, W.X.: The inverse scattering transform and soliton solutions of a combined modified Korteweg-de Vries equation. *J. Math. Anal. Appl.* **471**, 796–811 (2019)
- Bluman, G.W., Yang, Z.Z.: A symmetry-based method for constructing nonlocally related partial differential equation systems. *J. Math. Phys.* **54**, 093504 (2013)
- Wang, Y.H., Wang, H.: Nonlocal symmetry, CRE solvability and soliton-cnoidal solutions of the (2+1)-dimensional modified KdV-Calogero-Bogoyavlenskii-Schiff equation. *Nonlinear Dyn.* **89**, 235–241 (2017)
- Wang, X.B., Han, B.: Application of the Riemann-Hilbert method to the vector modified Korteweg-de Vries equation. *Nonlinear Dyn.* **99**, 1363–1377 (2019)

32. Wu, J.P., Geng, X.G.: Inverse scattering transform of the coupled Sasa-Satsuma equation by Riemann-Hilbert approach. *Commun. Theor. Phys.* **67**, 527–534 (2017)
33. Kumar, V., Gupta, R.K., Jiwari, R.: Lie group analysis, numerical and non-traveling wave solutions for the (2+1)-dimensional diffusion-advection equation with variable coefficients. *Chinese Phys. B* **23**(3), 030201 (2014)
34. Gupta, R.K., Kumar, V., Jiwari, R.: Exact and numerical solutions of coupled short pulse equation with time-dependent coefficients. *Nonlinear Dyn.* **79**, 455–464 (2015)
35. Kumar, S., Kumar, A.: Lie symmetry reductions and group invariant solutions of (2+1)-dimensional modified Veronese web equation. *Nonlinear Dyn.* **98**(3), 1891–1903 (2019)
36. Kumar, S., Kumar, A., Wazwaz, A.M.: New exact solitary wave solutions of the strain wave equation in microstructured solids via the generalized exponential rational function method. *Eur. Phys. J. Plus.* **135**(11), 870 (2020)
37. Liu, J.G., Yang, X.J., Geng, L.L., Yu, X.J.: On fractional symmetry group scheme to the higher dimensional space and time fractional dissipative Burgers equation. *Int. J. Geom. Methods M.* **19**(11), 2250173 (2022)
38. Wazwaz, A.M., El-Tantawy, S.A.: Solving the (3+1)-dimensional KP-Boussinesq and BKP-Boussinesq equations by the simplified Hirota's method. *Nonlinear Dyn.* **88**, 3017–3021 (2017)
39. Han, P.F., Bao, T.: Construction of abundant solutions for two kinds of (3+1)-dimensional equations with time-dependent coefficients. *Nonlinear Dyn.* **103**, 1817–1829 (2021)
40. Li, B.Q., Ma, Y.L.: Interaction dynamics of hybrid solitons and breathers for extended generalization of Vakhnenko equation. *Nonlinear Dyn.* **102**, 1787–1799 (2020)
41. Ablowitz, M.J., Satsuma, J.: Solitons and rational solutions of nonlinear evolution equations. *J. Math. Phys.* **19**, 2180–2186 (1978)
42. Satsuma, J., Ablowitz, M.J.: Two-dimensional lumps in nonlinear dispersive systems. *J. Math. Phys.* **20**, 1496–1503 (1979)
43. Li, B.Q., Ma, Y.L.: N-order rogue waves and their novel colliding dynamics for a transient stimulated Raman scattering system arising from nonlinear optics. *Nonlinear Dyn.* **101**, 2449–2461 (2020)
44. Ma, Y.L., Li, B.Q.: Kraenkel-Manna-Merle saturated ferromagnetic system: Darboux transformation and loop-like soliton excitations. *Chaos Solitons Fract.* **159**, 112179 (2022)
45. Yan, H., Tian, S.F., Feng, L.L., Zhang, T.T.: Quasi-periodic wave solutions, soliton solutions, and integrability to a (2+1)-dimensional generalized Bogoyavlensky-Konopelchenko equation. *Wave Random Complex* **26**(4), 444–457 (2016)
46. Guan, X., Liu, W.J., Zhou, Q., Biswas, A.: Some lump solutions for a generalized (3+1)-dimensional Kadomtsev-Petviashvili equation. *Appl. Math. Comput.* **366**, 124757 (2020)
47. Liu, S.H., Tian, B., Qu, Q.X., Li, H., Zhao, X.H., Du, X.X., Chen, S.S.: Breather, lump, shock and travelling-wave solutions for a (3+1)-dimensional generalized Kadomtsev-Petviashvili equation in fluid mechanics and plasma physics. *Int. J. Comput. Math.* **98**(6), 1130–1145 (2021)
48. Darvishi, M.T., Najafi, M., Kavitha, L., Venkatesh, M.: Stair and step soliton solutions of the integrable (2+1) and (3+1)-dimensional Boiti-Leon-Manna-Pempinelli equations. *Commun. Theor. Phys.* **58**, 785–794 (2012)
49. Xu, G.Q.: Painlevé analysis, lump-kink solutions and localized excitation solutions for the (3+1)-dimensional Boiti-Leon-Manna-Pempinelli equation. *Appl. Math. Lett.* **97**, 81–87 (2019)
50. Liu, J.G., Tian, Y., Hu, J.G.: New non-traveling wave solutions for the (3+1)-dimensional Boiti-Leon-Manna-Pempinelli equation. *Appl. Math. Lett.* **79**, 162–168 (2018)
51. Peng, W.Q., Tian, S.F., Zhang, T.T.: Breather waves and rational solutions in the (3+1)-dimensional Boiti-Leon-Manna-Pempinelli equation. *Comput. Math. Appl.* **77**(3), 715–723 (2019)
52. Wazwaz, A.M.: Painlevé analysis for new (3+1)-dimensional Boiti-Leon-Manna-Pempinelli equations with constant and time-dependent coefficients. *Int. J. Numer. Method. H.* **30**(9), 4259–4266 (2020)
53. Liu, J.G., Wazwaz, A.M.: Breather wave and lump-type solutions of new (3+1)-dimensional Boiti-Leon-Manna-Pempinelli equation in incompressible fluid. *Math. Methods Appl. Sci.* **44**, 2200–2208 (2021)
54. Yuan, N.: Rich analytical solutions of a new (3+1)-dimensional Boiti-Leon-Manna-Pempinelli equation. *Results Phys.* **22**, 103927 (2021)
55. Jimbo, M., Miwa, T.: Solitons and infinite dimensional Lie algebras. *Publ. Res. Inst. Math. Sci.* **19**, 943–1001 (1983)
56. Dai, Z.D., Li, Z.T., Liu, Z.J., Li, D.L.: Exact cross kink-wave solutions and resonance for the Jimbo-Miwa equation. *Phys. A* **384**, 285–290 (2007)
57. Wazwaz, A.M.: Multiple-soliton solutions for extended (3+1)-dimensional Jimbo-Miwa equations. *Appl. Math. Lett.* **64**, 21–26 (2017)
58. Sun, H.Q., Chen, A.H.: Lump and lump-kink solutions of the (3+1)-dimensional Jimbo-Miwa and two extended Jimbo-Miwa equations. *Appl. Math. Lett.* **68**, 55–61 (2017)
59. Guo, H.D., Xia, T.C., Hu, B.B.: High-order lumps, high-order breathers and hybrid solutions for an extended (3+1)-dimensional Jimbo-Miwa equation in fluid dynamics. *Nonlinear Dyn.* **100**, 601–614 (2020)
60. Wang, Y.H., Chen, Y.: Binary Bell polynomial manipulations on the integrability of a generalized (2+1)-dimensional Korteweg-de Vries equation. *J. Math. Anal. Appl.* **400**, 624–634 (2013)
61. Hirota, R.: *The direct method in soliton theory*. Cambridge University Press, New York (2004)
62. Li, B.Q., Ma, Y.L.: Extended generalized Darboux transformation to hybrid rogue wave and breather solutions for a nonlinear Schrödinger equation. *Appl. Math. Comput.* **386**, 125469 (2020)
63. Ma, W.X., Zhou, Y.: Lump solutions to nonlinear partial differential equations via Hirota bilinear forms. *J. Differ. Equ.* **264**, 2633–2659 (2018)
64. Zhao, Z.L., Chen, Y., Han, B.: Lump soliton, mixed lump stripe and periodic lump solutions of a (2+1)-dimensional asymmetrical Nizhnik-Novikov-Veselov equation. *Mod. Phys. Lett. B* **31**(14), 1750157 (2017)

65. Chen, S.J., Ma, W.X., Lü, X.: Bäcklund transformation, exact solutions and interaction behaviour of the (3+1)-dimensional Hirota-Satsuma-Ito-like equation. *Commun. Nonlinear Sci. Numer. Simul.* **83**, 105135 (2020)
66. Hu, C.C., Tian, B., Wu, X.Y., Yuan, Y.Q., Du, Z.: Mixed lump-kink and rogue wave-kink solutions for a (3+1)-dimensional B-type Kadomtsev-Petviashvili equation in fluid mechanics. *Eur. Phys. J. Plus* **133**, 40 (2018)
67. Han, P.F., Bao, T.: Interaction of multiple superposition solutions for the (4+1)-dimensional Boiti-Leon-Manna-Pempinelli equation. *Nonlinear Dyn.* **105**, 717–734 (2021)
68. Han, P.F., Bao, T.: Dynamic analysis of hybrid solutions for the new (3+1)-dimensional Boiti-Leon-Manna-Pempinelli equation with time-dependent coefficients in incompressible fluid. *Eur. Phys. J. Plus* **136**, 925 (2021)

Publisher's Note Springer Nature remains neutral with regard to jurisdictional claims in published maps and institutional affiliations.

Springer Nature or its licensor (e.g. a society or other partner) holds exclusive rights to this article under a publishing agreement with the author(s) or other rightsholder(s); author self-archiving of the accepted manuscript version of this article is solely governed by the terms of such publishing agreement and applicable law.